A Search for Lorentz and CPT Violation Using the T2K Near Detectors

Gary Alexander Clifton[1]

[1]Colorado State University, Fort Collins, Colorado USA

DOI: http://dx.doi.org/10.3204/DESY-PROC-2016-05/36

Lorentz symmetry violation (LV) arises when the behavior of a particle depends on its direction or boost velocity. The Standard Model Extension (SME) is a general theoretical framework that includes both General Relativity and the Standard Model while also allowing for the breaking of particle Lorentz symmetry through a set of controlling coefficients. A search for LV at the T2K near detectors with baselines of 280 m is described. The protons-on-target normalized neutrino event rate at the T2K near detectors is used to search for LV using a shape-only analysis via Fast Fourier Transform (FFT) analysis and a binned log-likelihood fit. No indication of LV is observed with either method in the T2K near detector data.

1 Conventional Neutrino Oscillations

For non-interacting neutrinos, the Hamiltonian eigenstates are the mass eigenstates and the mixing matrix is then equated to the Pontecorvo, Maki, Nakagawa, and Sakata (PMNS) matrix. The PMNS matrix may be parameterized with three mixing angles $(\theta_{12}, \theta_{23}, \theta_{13})$ and one complex phase factor (δ_{CP}). The probability of neutrino flavor oscillation in natural units is

$$\begin{aligned} P_{\nu_\alpha \to \nu_\beta}(L) =& \delta_{\alpha\beta} - 4 \sum_{i>j} \mathrm{Re}(U^*_{\alpha i} U_{\beta i} U_{\alpha j} U^*_{\beta j}) \sin^2(\frac{\Delta m^2_{ij}}{4E} L) \\ &+ 2 \sum_{i>j} \mathrm{Im}(U^*_{\alpha i} U_{\beta i} U_{\alpha j} U^*_{\beta j}) \sin(\frac{\Delta m^2_{ij}}{2E} L) \end{aligned} \tag{1}$$

where

$$\Delta m^2_{ij} = m^2_i - m^2_j \tag{2}$$

is the mass-squared splitting, $U_{\gamma k}$ are the elements of the PMNS matrix, L is the baseline of the neutrino experiment, and E is the neutrino energy. Thus, conventionally, neutrino oscillations are driven by a unique neutrino mass.

2 T2K Experiment

T2K utilizes a 2.5° off-axis neutrino beam for optimal detection of ν_e appearance at a peak neutrino energy of 0.6 GeV with a baseline of 295km at the Super Kamiokande far detector.

The experiment consists of a ν_μ beam produced at the JPARC facility in Tokai, Japan, near detector site, and a far detector site. An on-axis near detector, called the interactive neutrino grid (INGRID), monitors the beam stability and intensity while the off-axis near detector, called the near detector at 280m (ND280), is used to study neutrino interactions for different nuclear targets as well as study neutrino kinematics. Both near detectors are located at 280m from the graphite target used to create the T2K neutrino beam.

2.1 INGRID

INGRID was designed to measure the beam intensity and direction by utilizing neutrino interactions on iron [1] and lies on axis at 280m from the graphite target [2]. INGRID is arranged in a cross configuration with 14 identical modules [4] to detect neutrino interactions from the beam. In addition to these 14 modules, two shoulder modules exist to check the axial symmetry of the neutrino beam. Each module consists of alternating layers of scintillator and iron plates. In each module, there are 11 scintillator tracking planes that consist of 24 horizontal and 24 vertical scintillator bars glued together.

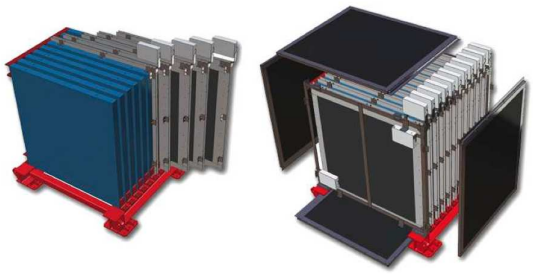

Figure 1: A diagram showing the layout of an INGRID module.

2.2 ND280

ND280 was designed to perform several measurements [2]:

1. Measure the neutrino flux and energy from the beam
2. Measure the inherent ν_e contamination of the beam
3. Measure neutrino event rates

It is a composite detector encased in the UA1 dipole magnet. The π^0 detector, or P0D, [7] was constructed to measure the following neutral current interaction on a water target:

$$\nu_\mu + N \rightarrow \nu_\mu + N + \pi^0 + X \tag{3}$$

Downstream of the P0D are three time projection chambers (TPCs). The TPCs measure the charge, momentum, and particle types of the different charged particles that are produced in neutrino interactions below a few GeV [2]. Each TPC consists of an inner and outer box [9]. The inner box contains an argon gas mixture for charged particles to ionize during their interactions.

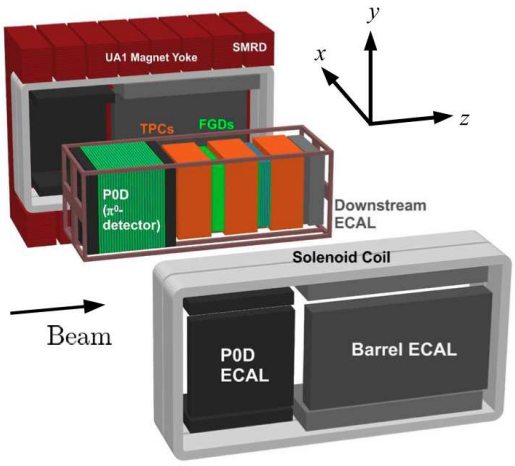

Figure 2: A blowout diagram of ND280 showing the different sub-detectors.

The outer box contains a CO_2 atmosphere which provides electrical insulation between the inner box and ground while also keeping atmospheric oxygen from entering the inner box. In addition to the P0D, two Fine Grained Detectors (FGD) were installed to provide a target for studying neutrino interactions as well as tracking of charged particles [8]. Each FGD consists of finely segmented scintillator bars arranged in X and Y planes. The electromagnetic calorimeters (ECals) of ND280 are sampling calorimeters located inside the magnet yokes and enclose the various subdetectors of ND280 (P0D, TPCs, FGDs). The ECals serve to measure the energy and direction of charged particles that exit the sides of the ND280 subdetectors in order to identify particle types [5]. Each ECal module consists of alternating layers of scintillator bars and lead sheets. The Side Muon Range Detector (SMRD) system is located between the air gaps in each magnet yoke and uses scintillator planes to detect high angle muons that escape ND280 with respect to the beam line and measure their momentum [6].

3 The Standard Model Extension

The Standard Model Extension (SME) is a general theoretical framework conceived to facilitate experimental investigations of LV and CPT violation (CPTV) [3]. It is an effective field theory that contains General Relativity, the Standard Model, and all possible Lorentz violating operators. The SME allows for the breaking of Particle Lorentz symmetry which produces a tensor background field that permeates throughout the universe. Neutrinos couple to this background field with some given strength and the physics that the SME predicts becomes dependent, for example, on the absolute direction of neutrino propagation. This dependency can produce a number of effects, namely sidereal variations. LV is controlled by a set of coefficients which experiments may measure while working in the sun centered inertial frame. The probability of oscillation in the SME at short baselines is given by

$$P(\nu_\mu \to \nu_x) = L^2 |\mathcal{C}_{\mu x} + (\mathcal{A}_s)_{\mu x} \sin(\omega_\oplus T_\oplus) + (\mathcal{A}_c)_{\mu x} \cos(\omega_\oplus T_\oplus) + (\mathcal{B}_s)_{\mu x} \sin(2\omega_\oplus T_\oplus) + (\mathcal{B}_c)_{\mu x} \cos(2\omega_\oplus T_\oplus)|^2 \quad (4)$$

where $\omega_\oplus$ is the Earth's sidereal frequency and $T_\oplus$ is the sidereal time of the neutrino event in the detector. The various amplitudes associated with each sidereal time harmonic consist of the SME coefficients $(a_L)^\alpha_{\mu x}$ and $(c_L)^{\alpha\beta}_{\mu x}$, the neutrino energy E, and geographical information about how the neutrino beam is setup on Earth. Thus, in the SME, neutrino oscillations vary with sidereal time producing a sidereal variation in the neutrino event rate at a given detector.

4 LV Analysis

To perform a LV search at the T2K near detectors, T2K data taken from 2010 to 2013 is used. This data was taken in various T2K data run periods throughout this time. For INGRID, all the data is combined into a single data sample, while for ND280 since the P0D can be configured with or without water, two data samples are used corresponding to each configuration of the P0D. The POT normalized neutrino event rate as a function of Local Sidereal Phase (LSP) for each data set is shown in Figures 3.

$$LSP = mod\Big(\frac{T_\oplus}{23^h 56^m 4.0916^s}\Big) \quad (5)$$

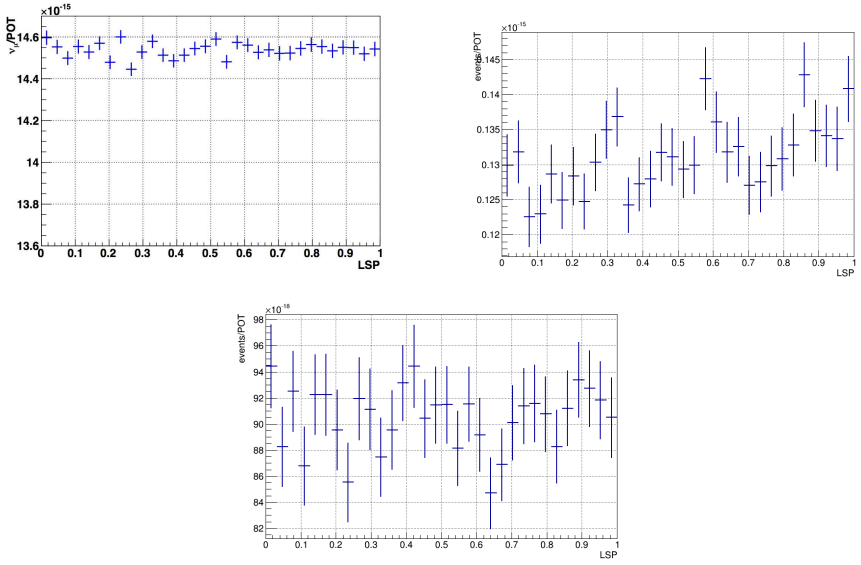

Figure 3: Corrected ν_μ event rate versus LSP in INGRID (top left), ND280 water-in (top right), and ND280 water-out (bottom).

Each data set consists of 32 LSP bins to avoid aliasing effects in the Fast Fourier Transform method (described below). Each data sample was analyzed for various sources of systematic

uncertainty that could mimic a LV signal. All sources of systematic error were found to be negligible compared to statistical uncertainty and corrections were calculated for each source and applied to the data.

The analysis is broken up into two parts: a Fast Fourier Transform (FFT) method and a binned likelihood fit method. The FFT method is applied to both INGRID and ND280 data while only the INGRID data is used to perform the binned likelihood fit as it is a significantly higher statistical sample.

4.1 Fast Fourier Transform Method

A set of 10,000 data-driven toy experiments is created for which any potential LV signal is removed by randomizing the various LSP bins for a given sample based off the total number of beam spills in that sample. An example is shown in Figure 4.

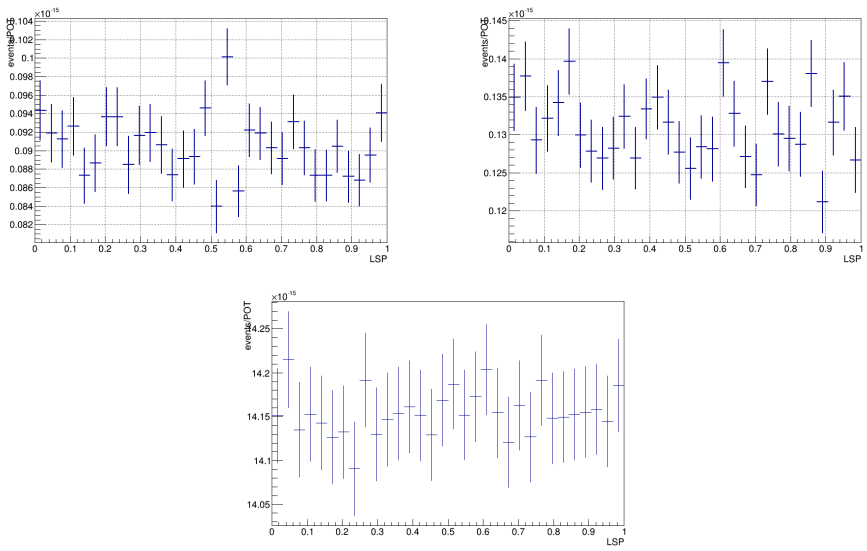

Figure 4: Examples of a ND280 flat toy MC for the water-in and water-out samples (left, middle) and an INGRID flat toy MC (right).

For a given detector, each toy is passed to a FFT tool which calculates the magnitude of the FFT. As such, a distribution of magnitude values for a given Fourier mode can be created for each detector. Such a distribution is shown in Figure 5. A 99.7% confidence level hypothesis test is performed to determine the significance of the FFT values in data. An overall detection threshold is calculated from the Fourier mode distributions of each Fourier mode as the largest detection threshold. A p-value is calculated utilizing the value observed in data, the Fourier mode distributions, and the total number of toy MC.

The corrected INGRID, ND280 water-in, an ND280 water-out ν_μ event rate as a function of LSP was analyzed with the method described above. The results of the FFT analysis can be

seen in Figure 6, Table 1, Table 2, and Table 3. The Fourier modes of interest to this analysis are below the 3σ detection threshold.

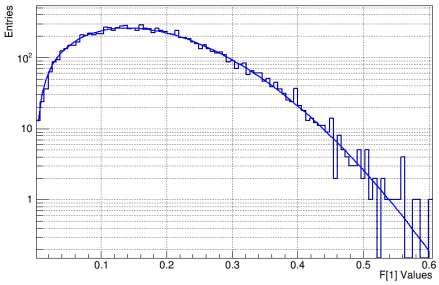

Figure 5: Distribution of the magnitude of the first Fourier mode for the 10,000 flat toy experiments of ND280 water-out. The distribution is fitted with a Rayleigh function.

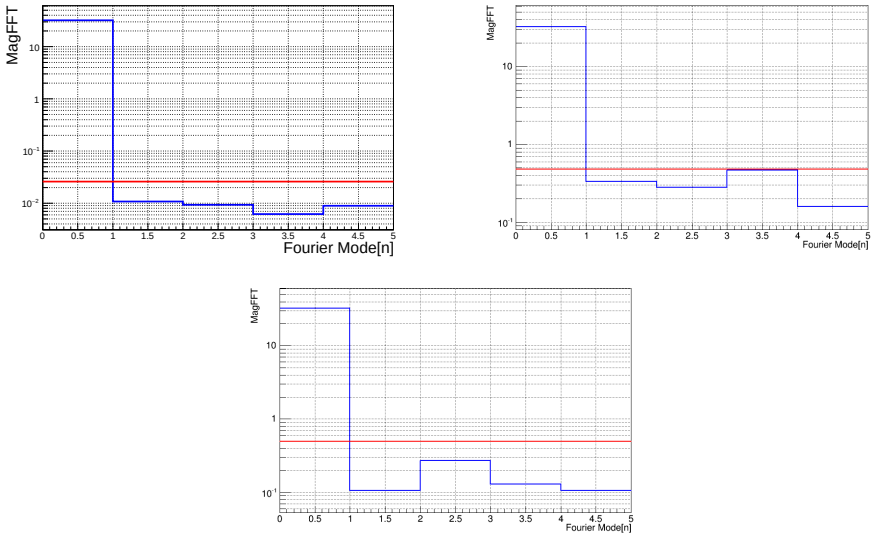

Figure 6: Magnitude of each Fourier mode in case of INGRID data (left), ND280 water-in (middle) data, and water-out (right) data after all corrections. The red horizontal line corresponds to the overall 3σ detection threshold.

Fourier Mode	Threshold	Magnitude	p-value
1	0.026	0.01076	0.35
2	0.026	0.00930	0.48
3	0.026	0.00620	0.69
4	0.026	0.00893	0.51

Table 1: FFT results for INGRID.

Fourier Mode	Threshold	Magnitude	p-value
1	0.4765	0.33537	0.055
2	0.4765	0.28221	0.126
3	0.4765	0.46355	0.004
4	0.4765	0.15999	0.511

Table 2: FFT results for ND280 water-in.

Fourier Mode	Threshold	Magnitude	p-value
1	0.4947	0.10501	0.765
2	0.4947	0.26948	0.162
3	0.4947	0.12856	0.659
4	0.4947	0.10649	0.751

Table 3: FFT results for ND280 water-out.

While the third Fourier mode p-value in the water-in sample is larger than the significance (0.003), it is still very close to it. If this were truly a LV effect in this data sample, this effect is expected to appear in the other samples. Since it does not, this affect is attributed to a statistical fluctuation. Thus, it is concluded that the INGRID, ND280 water-in, and ND280 water-out data are consistent with no sidereal variation in the relevant Fourier modes using the FFT analysis method. 99.7%C.L. upper limits on the SME coefficients may be extracted for the each sample utilizing the following procedure:

1. Set all but one SME coefficient to zero
2. Increase the size of the SME coefficient in a set of 10,000 signal toy Monte-Carlo until the nominal threshold has been crossed
3. Take the corresponding value of the coefficient as the upper limit

The 99.7%C.L. upper limits of the SME coefficients in each sample using this procedure are shown in Table 4.

Coefficient	ND280 Water-in	ND280 Water-out	INGRID
a_L^T	-	-	-
a_L^X	15.7 GeV	15.4GeV	4.8 GeV
a_L^Y	16.3 GeV	17.4GeV	4.8 GeV
a_L^Z	-	-	-
c_L^{TT}	-	-	-
c_L^{TX}	13.9	10.8	0.9
c_L^{TY}	13.9	13.0	0.9
c_L^{TZ}	-	-	-
c_L^{XX}	54.0	57.0	3.8
c_L^{XY}	25.0	25.0	1.6
c_L^{XZ}	-	-	3.1
c_L^{YY}	54.0	57.0	3.8
c_L^{YZ}	-	-	3.1
c_L^{ZZ}	-	-	-

Table 4: Standard Model Extension 3σ upper limits on SME coefficients related to $\nu_\mu \rightarrow \nu_e$ oscillation, for ND280 water-in and water-out, and INGRID (all values given in $\times 10^{-20}$).

4.2 Binned Likelihood Method

Due to the large degree of correlation, a five coefficient binned likelihood fit was developed instead of a full fourteen-coefficient to extract limits on the SME coefficients. The five coefficients are the amplitudes associated with each sidereal time harmonic in Equation 4. A binning of 32 bins in LSP was chosen for the likelihood fit, just as in the FFT method. For each LSP bin, the statistical errors are assumed to be Gaussian and the likelihood may be constructed as:

$$L = \prod_{i=1}^{32} e^{-\frac{(d_i - m_i)^2}{2\sigma_i^2}} \tag{6}$$

where, d_i and m_i are the POT normalized number of events in the i^{th} LSP bin for data and toy MC respectively, and

$$\sigma_i = \frac{N_{\nu_\mu}}{N_{\mathrm{POT}}} \sqrt{\frac{\delta N_{\nu_\mu}^2}{N_{\nu_\mu}^2} + \frac{\delta N_{\mathrm{POT}}^2}{N_{\mathrm{POT}}^2}}, \tag{7}$$

with N_{ν_μ} and N_{POT} being, respectively, the number of neutrino events and the number of protons on target in LSP bin i, with δN_{ν_μ} and δN_{POT} the corresponding statistical errors. The fitter was run over the corrected INGRID data. Table 5 shows the best fit values for each coefficient.

	$(\mathcal{C})_{ab}$	$(\mathcal{A}_s)_{ab}$	$(\mathcal{A}_c)_{ab}$	$(\mathcal{B}_s)_{ab}$	$(\mathcal{B}_c)_{ab}$
Best fit (10^{-20} GeV)	$-0.61^{+2.63}_{1.41}$	$0.38^{+1.83}_{-2.60}$	$-1.55^{+4.55}_{-1.44}$	$0.06^{+0.87}_{-1.00}$	$0.38^{+0.80}_{-1.57}$

Table 5: Best fit values with 1σ errors, and 2σ upper limit values on the different Standard Model Extension coefficients using the likelihood method.

All limits set by INGRID are consistent with zero (i.e. no LV) to 1σ.

5 Summary

The near detectors of T2K were used to search for indications of LV in the neutrino data. The two methods utilized (FFT method and binned likelihood fit) show that all data sets used are consistent with the null hypothesis, namely, no sidereal variations. Figure 7 compares the results using the FFT method of INGRID and ND280 with MiniBooNE and MINOS (left) and the results of the likelihood method for INGRID and MiniBooNE (right). For the likelihood, all limits set by INGRID are consistent with no LV to 1σ. $(\mathcal{B}_s)_{ab}$ and $(\mathcal{B}_c)_{ab}$ have now been constrained in INGRID as they previously were not.

	Upper limits (10^{-20})				
SME Coeff.	MiniBoonE	MINOS	INGRID	ND280 Water-in	ND280 Water-out
a_L^T	4.2 GeV	-	-	-	-
a_L^X	6.0 GeV	2.2 GeV	4.8 GeV	15.7 GeV	15.4 GeV
a_L^Y	5.0 GeV	2.2 GeV	4.8 GeV	16.3 GeV	17.4 GeV
a_L^Z	5.6 GeV	-	-	-	-
c_L^{TT}	9.6	-	-	-	
c_L^{TX}	8.4	0.009	0.9	13.9	10.8
c_L^{TY}	6.9	0.009	0.9	13.9	13.0
c_L^{TZ}	7.8	-	-	-	-
c_L^{XX}	-	0.46	3.8	54.0	57.0
c_L^{XY}	-	0.22	1.6	25.0	25.0
c_L^{XZ}	11	0.11	3.1	-	-
c_L^{YY}	-	0.45	3.8	54.0	57.0
c_L^{YZ}	9.2	0.11	3.1	-	-
c_L^{ZZ}	34	-	-	-	-

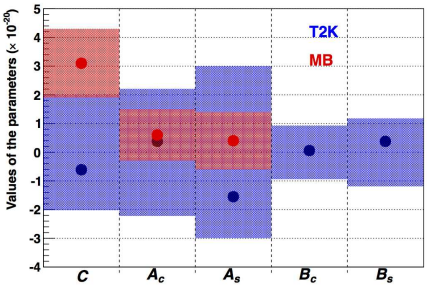

Figure 7: Comparison of SME Coefficients associated with ν_e appearance INGRID and ND280 with other experiments using the FFT method (left) and comparison between the T2K (blue) and MiniBooNE (red) best fit values and 1σ limits (right).

It should be stressed that this level of precision is still very valuable to theorists. T2K probes a different direction in the Sun-centered reference frame, and thus samples a different portion of the coefficient space. This information helps theorist improve their theories so that experimentalists may continue to test them.

6 Aknowledgements

I thank the J-PARC team for the superb accelerator performance and CERN NA61 colleagues for providing particle production data. I acknowledge the support of the US Department of Energy for my research. Finally, I want to thank the organizers of the Magellan Workshop for giving me the opportunity to present.

References

[1] T. Le *et al.* Overview of the T2K long baseline neutrino oscillation experiment, Proceedings of the DPF-2009 Conference (2009).

[2] K. Abe *et al.* Nuclear Instruments and Methods in Physics **69** 106 (2011).

[3] D. Colladay, A. Kostelecky Phys. Rev. D. **58** 116002 (1998).

[4] K. Abe *et al.* Nuclear Instruments and Methods in Physics. "Measurements of the T2K neutrino beam properties using the INGRID on-axis near detector" **A694** (2012).

[5] D Allan *et al.* JINST. "The Electromagnetic Calorimeter for the T2K Near Detector ND280" **8** (2013).

[6] S. Aoki *et al.* Nuclear Instruments and Methods in Physics. "The T2K Side Muon Range Detector" **A698** (2013).

[7] S. Assylbekov *et al* Nuclear Instruments and Methods in Physics. "The T2K ND280 Off-Axis Pi-Zero Detector" **A686** (2012).

[8] P.-A. Amaudruz *et al* Nuclear Instruments and Methods in Physics. "The T2K Fine-Grained Detectors" **A696** (2012).

[9] N. Abgrall *et al* Nuclear Instruments and Methods in Physics. "Time Projection Chambers for the T2K Near Detectors" **A637** (2011).